

## A Theoretical Study of the HO<sub>2</sub> + HN<sub>2</sub> Reaction

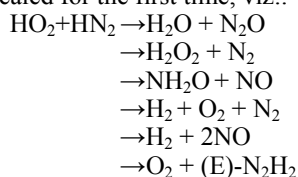
Tiancheng Xiang \*, Hongyan Si, Yanru Zhao  
 School of Chemistry and Chemical Engineering  
 Xuchang University  
 Xuchang, China  
 xtc7828@163.com

**Abstract**—The mechanism of the HO<sub>2</sub> + HN<sub>2</sub> reaction has been investigated at the B3LYP/6-311++G (3df, 3pd) level. The single-point energy calculations are performed at the high-level CCSD (T) / 6-311++G (3df, 3pd) for more accurate energy values. For the HO<sub>2</sub> + HN<sub>2</sub> reaction, DFT calculations show the dissociation of im4 leading to N<sub>2</sub>O + H<sub>2</sub>O is predominant on the singlet energy surface, and the N<sub>2</sub> + H<sub>2</sub>O<sub>2</sub> are expected to be secondary products.

**Keywords**—DFT calculations; reaction mechanism; HO<sub>2</sub> radical; HN<sub>2</sub> radical

### I. INTRODUCTION

As a very reactive species, HO<sub>2</sub> radical has been subjected to wide investigations in atmospheric chemistry and combustion chemistry<sup>[1-6]</sup>. HN<sub>2</sub> radical also should be taken into consideration as an important reactive intermediate in the generation of NO<sup>[7-10]</sup>. As a possible pathway to product or reduce NO, the radical-radical reaction of HO<sub>2</sub> with HN<sub>2</sub> must be interested in the combustion chemistry and atmospheric chemistry. Unfortunately it is lack of the knowledge of products, pathway and mechanism of this reaction in the literatures so far. In this paper, the energetic of the reaction pathways for the HO<sub>2</sub> + HN<sub>2</sub> reaction has been investigated by ab initio method on the singlet energy surface. The mechanisms for the exothermic product channels are revealed and the endothermic channels are discarded. For the HO<sub>2</sub>+HN<sub>2</sub> reaction, the following exothermic product channels are revealed for the first time, viz.:



### II. CALCULATION METHOD

The ab initio calculations were carried out by the Gaussian03 program package<sup>[11]</sup>. The geometries of the reactants, products, intermediates and transition states were optimized using DFT calculations at the B3LYP/6-311++G (3df, 3pd) level. The reaction paths are checked by performing intrinsic reaction coordinate (IRC) calculation<sup>[12]</sup>, from which the quadratic steepest descent reaction paths are confirmed to connect the corresponding minima at the same level. In order to obtain more reliable energies, the single-

point energy calculations were performed at the high-level CCSD (T) / 6-311++G (3df, 3pd).

### III. RESULTS AND DISCUSSION

Energies and geometries of the reactants, intermediates and transition states are calculated and shown in Fig. 1 to Fig. 2. The total energy of the reactants is set as zero, and the relative energies of all species involved in the studied reaction are listed in Table 1. In Table 1, comparison with experimental results shows that the calculational results for the HO<sub>2</sub> + HN<sub>2</sub> reaction are accurate. So the present level of calculations can provide reliable energetic and mechanistic information for the reaction of HO<sub>2</sub> with HN<sub>2</sub>.

Table 1 Zero-Point, Total (au), and Relative Energies(kJ.mol<sup>-1</sup>) of Reactant, Products, and Isomers for the HO<sub>2</sub> + HN<sub>2</sub> Reaction at the CCSD (T) / 6-311++G (3df, 3pd) Level.

species	ZPE	CCSD (T)	CCSD (T)+ZPE	$\Delta H_{298}^a$
HO <sub>2</sub> + HN <sub>2</sub>	0.02735	-260.58025	0	
O <sub>2</sub> +N <sub>2</sub> H <sub>2</sub>	0.03208	-260.60882	-62.6	
H <sub>2</sub> +2NO	0.01907	-260.60712	-92.3	-82.3
NH <sub>2</sub> O+NO	0.03095	-260.62589	-110.4	
H <sub>2</sub> +N <sub>2</sub> +O <sub>2</sub>	0.01937	-260.67388	-266.7	-262.9
N <sub>2</sub> +H <sub>2</sub> O <sub>2</sub>	0.03214	-260.73421	-391.6	-399.0
H <sub>2</sub> O+N <sub>2</sub> O	0.03250	-260.74536	-419.9	-422.7
im11	0.03498	-260.60136	-35.4	
im12	0.03587	-260.62361	-91.5	
im13	0.03543	-260.62321	-91.6	
im14	0.03553	-260.62812	-104.2	
im15	0.03667	-260.63077	-108.2	
im16	0.03638	-260.55562	88.4	
im17	0.03893	-260.66410	-189.7	
im18	0.03693	-260.66732	-203.4	
im19	0.03827	-260.63180	-106.7	
ts11	0.03197	-260.54562	103.0	
ts12	0.03227	-260.54889	95.3	
ts13	0.02437	-260.55799	50.6	
ts14	0.03134	-260.58088	8.8	
ts15	0.03345	-260.59399	-20.1	
ts16	0.03359	-260.59491	-22.1	
ts17	0.03221	-260.59978	-38.5	
ts18	0.03199	-260.60204	-45.0	
ts19	0.03302	-260.53572	131.8	
ts20	0.03268	-260.56219	-61.4	
ts21	0.03135	-260.56464	51.5	
ts22	0.03135	-260.59111	-18.0	
ts23	0.02533	-260.52764	132.8	

a. The formation enthalpies are taken from [13], [14]

As shown in Figure 1, there are five adducts come from the initial association. The intermediate im1 is obtained by the barrierless addition of the HOO to HN(N) radicals, which is 35.4kJ.mol<sup>-1</sup> more stable than the separate reactants. The attack of HOO at the terminal nitrogen atom of the

HNN form the adduct HNN-OOH in four conformations (im2, im3, im4, im5), which with association energy of  $-91.5 \text{ kJ}\cdot\text{mol}^{-1}$ ,  $-91.6 \text{ kJ}\cdot\text{mol}^{-1}$ ,  $-104.2 \text{ kJ}\cdot\text{mol}^{-1}$  and  $-108.2 \text{ kJ}\cdot\text{mol}^{-1}$ , respectively. These adducts can be product directly from the reactants. After the initial addition, the energized adducts undergo subsequent isomerization steps forming a variety of intermediates and products.

From these adducts, there are four direct dissociation routes. For example, im1 can be rearranged to lead the product  $\text{N}_2 + \text{H}_2\text{O}_2$  depending on the H transfer from the N atom to the O atom by surmounting a fairly low barrier of  $44.2 \text{ kJ}\cdot\text{mol}^{-1}$ . Analogously, the routes  $\text{R} \rightarrow \text{im3} \rightarrow \text{ts7} \rightarrow (\text{N}_2 + \text{H}_2\text{O}_2)$ ,  $\text{R} \rightarrow \text{im4} \rightarrow \text{ts3} \rightarrow (\text{H}_2 + \text{N}_2 + \text{O}_2)$  and  $\text{R} \rightarrow \text{im4} \rightarrow \text{ts8} \rightarrow (\text{N}_2\text{O} + \text{H}_2\text{O})$  are also directly dissociation by surmounting the barrier of  $53.1 \text{ kJ}\cdot\text{mol}^{-1}$ ,  $154.8 \text{ kJ}\cdot\text{mol}^{-1}$  and  $49.2 \text{ kJ}\cdot\text{mol}^{-1}$ , respectively. Among these four pathways, the dissociation of im4 to  $\text{N}_2\text{O} + \text{H}_2\text{O}$  should be dominant because its transition state lies at  $45.0 \text{ kJ}\cdot\text{mol}^{-1}$  below the reactant. This value is lower than the barriers to the other product channels. Because the barrier of the channel is below the reactants, the products of  $\text{N}_2 + \text{H}_2\text{O}_2$  are also possible.

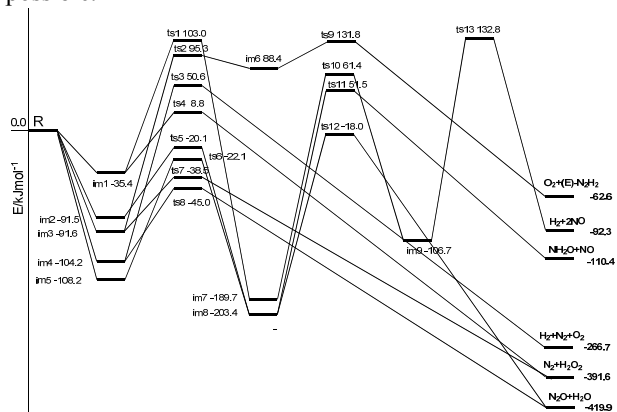


Figure 1 Energy diagram for the  $\text{HO}_2 + \text{HN}_2$  reaction paths on the singlet surface.

There are three possible pathways to product NO in the  $\text{HO}_2 + \text{HN}_2$  reaction on the singlet potential surface. One channel leads to  $\text{H}_2 + 2\text{NO}$  from im1, another two channels yield the products of  $\text{NH}_2\text{O} + \text{NO}$  from im2 or im5. Starting from im1, An OH transfer from C to N atom of im1 requires overcoming a high barrier of  $138.4 \text{ kJ}\cdot\text{mol}^{-1}$ , leading to the intermediate im7. Im7 could isomerize to intermediate im9 by H transfer from O to N atom over a high barrier of  $251.1 \text{ kJ}\cdot\text{mol}^{-1}$ . Sequentially, the Cleavage of the N-N bond accompany with the linking of two H atom of the intermediate im9, gives rise to the final products of  $\text{H}_2 + 2\text{NO}$ . Obviously it is difficult to surmount three higher barriers in low-temperature condition. So from the dynamical view, the path is negligible. The products of  $\text{NH}_2\text{O} + \text{NO}$  can be obtained from im8 via a transition state of ts11 with a fairly high barrier of  $254.9 \text{ kJ}\cdot\text{mol}^{-1}$ . Two isomerization routes to lead the intermediate im8 have been found. The first route comes from im2 via a transition state ts5 with a barrier of  $71.4 \text{ kJ}\cdot\text{mol}^{-1}$ . The second route is the rearrangement of im5 through a transition state ts6 by surmounting the barrier of  $86.1 \text{ kJ}\cdot\text{mol}^{-1}$ . Because of a higher

barrier in the pathways, the corresponding products of  $\text{NH}_2\text{O} + \text{NO}$  are not important on the singlet potential surface

The dissociation of im8 is another possible pathway to lead the products of  $\text{N}_2\text{O} + \text{H}_2\text{O}$ . This process requires overcoming a barrier of  $185.4 \text{ kJ}\cdot\text{mol}^{-1}$ .

From im3, there is an H transfer route leading to the intermediate im6 via a transition state of ts2 with a fairly high barrier of  $186.9 \text{ kJ}\cdot\text{mol}^{-1}$ . The subsequent Cleavage of N-O bond in im6 requires overcoming a low barrier of  $43.4 \text{ kJ}\cdot\text{mol}^{-1}$ , yielding the products of  $\text{O}_2 + (\text{E})\text{-N}_2\text{H}_2$ . Compared with other energy reaction routes, the path must surmount two higher energy barriers and is less favorable.

Other reaction routes have also been explored for the  $\text{HO}_2 + \text{HN}_2$  reaction. For example, there should also be a channel producing  $\text{N}_2 + 2\text{OH}$ . The calculations show that the  $\text{N}_2 + 2\text{OH}$  can be obtained from the product  $\text{N}_2 + \text{H}_2\text{O}_2$  via the further dissociations of  $\text{H}_2\text{O}_2$ . And the products of  $\text{O}_2 + (\text{Z})\text{-N}_2\text{H}_2$  can also be product from the product  $\text{O}_2 + (\text{E})\text{-N}_2\text{H}_2$  thought the further isomerization of  $(\text{E})\text{-N}_2\text{H}_2$ . Due to the result is irrelevant to the mechanism discussion and thus not depicted in Figure 4.

As can be seen from the above discussion and from Figure 1, the dissociation of im4 leading to  $\text{N}_2\text{O} + \text{H}_2\text{O}$  is predominant on the singlet energy surface for the  $\text{HO}_2 + \text{HN}_2$  reaction because of its lowest barrier height of  $45.0 \text{ kJ}\cdot\text{mol}^{-1}$  below the reactant, whereas  $\text{N}_2 + \text{H}_2\text{O}_2$  are expected to be secondary products. The other channels may play a minor or negligible role in the reaction.

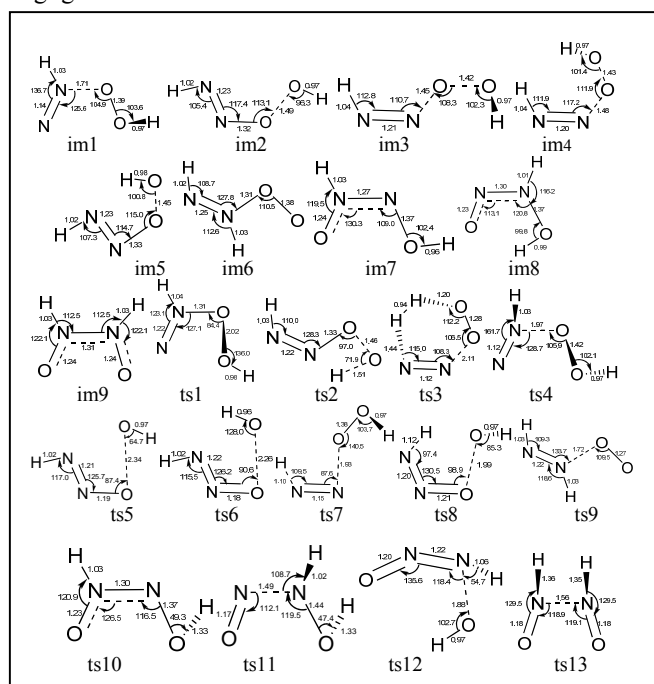


Figure 2 Optimized structures of transition states and intermediates (bond length in angstrom and angle in degree) at the B3LYP/6-311++G(3df,3pd) level along the singlet channels for the  $\text{HO}_2 + \text{HN}_2$  reaction.

#### IV. CONCLUSIONS

A detailed singlet potential energy surface calculation of the HO<sub>2</sub> + HN<sub>2</sub> reaction system has been carried out at the B3LYP/6-311++G (3df, 3pd) and CCSD (T) (single-point) levels. For the HO<sub>2</sub> + HN<sub>2</sub> reaction, DFT calculations show that the reaction proceeds through the isomerization and decomposition of the initially formed adducts HNN-OOH on the singlet potential surface. The dissociation of im4 leading to N<sub>2</sub>O + H<sub>2</sub>O is predominant on the singlet energy surface.

#### ACKNOWLEDGMENT

This work is supported by the National Natural Science Foundation of China (Grant No. 21107090) and the Natural Science Foundation of Education Department of Henan Province (No. 2009b15002).

#### REFERENCES

- [1] D. E. Heard, M. J. Pilling. Measurement of OH and HO<sub>2</sub> in the troposphere. *Chem. Rev.*, vol. 103, Dec. 2003, pp. 5163-5198. doi: 10.1021/cr020522s.
- [2] Y. Bedjanian, G. Poulet, Kinetics of halogen oxide radicals in the stratosphere, *Chem. Rev.*, vol. 103, Dec. 2003, pp. 4639-4655. doi: 10.1021/cr0205210.
- [3] R. Atkinson, D. L. Baulch, et al. Evaluated kinetic and photochemical data for atmospheric chemistry: Volume I - gas phase reactions of Ox, HOx, NOx and SOx species. *Atmos. Chem. Phys.*, vol. 4, Sep, 2004, pp. 1461-1738.
- [4] R. S. Zhu, M. C. Lin. Ab initio chemical kinetics for ClO reactions with HOx, ClOx and NOx (x = 1, 2): A review. *Comput. Theor. Chem.*, vol. 965, 2011, pp. 328-339. doi: 10.1016/j.comptc. 2010. 12. 002.
- [5] J. P. Le Crane, M. T. Rayez, J. C. Rayez, Eric Villenave, A reinvestigation of the kinetics and the mechanism of the CH<sub>3</sub>C(O)O<sub>2</sub> + HO<sub>2</sub> reaction using both experimental and theoretical approaches, *Phys. Chem. Chem. Phys.*, vol. 8, 2006, pp. 2163-2171. doi: 10.1039/B518321A.
- [6] P. J. S. B. Caridade, S. P. J. Rodrigues, F. Sousa, and A. J. C. Varandas. Unimolecular and bimolecular calculations for HN<sub>2</sub>. *J. Phys. Chem. A*, vol. 109, Feb 2005, pp. 2356-2363. doi: 10.1021/jp045102g.
- [7] N. L. Haworth, J. C. Mackie, G. B. Bacskay. An ab initio quantum chemical and kinetic study of the NNH + O reaction potential energy surface: How important is this route to NO in combustion? *J. Phys. Chem. A*, vol. 107, Aug 2003, pp. 6792-6803. doi: 10.1021/jp034421p.
- [8] A. A. Konnov, De Ruyck, Temperature-Dependent rate constant for the reaction NNH + O -> NH + NO. *Combust. Flame*, vol. 125, 2001, pp. 1258-1264. doi: 10.1016/S0010-2180(01)00250-4.
- [9] T. C. Xiang, Y. R. Zhao, J. L. Xu, A theoretical study of the 2NCO + 2N<sub>2</sub>H reaction. *J. Mol. Struct: Theochem*, vol. 958, 2001, pp. 958(2010) 10-14. doi: 10.1016/j.theochem.2010.07.019.
- [10] J. W. Bozzelli, A. M. Dean. O - NNH: a possible new route for NOx formation in flames. *Int. J. Chem. Kinet.*, vol. 27, 1995, pp. 1097-1109. doi: 10.1002/kin.55027110.
- [11] M. J. Frisch, G.W. Trucks, et al. Gaussian 03, Revision E.01, Gaussian, Inc., Wallingford, CT, 2004.
- [12] C. Gonzalez, H. B. Schlegel. Reaction path following in mass-weighted internal coordinates. *J. Phys. Chem.*, vol. 94, July 1990, pp. 5523-5527. doi: 10.1021/j100377a021.
- [13] M. W. Jr. Chase. NIST-JANAF Thermochemical Tables, Fourth Edition, *J. Phys. Chem. Ref. Data.*, vol. 9, 1998, pp. 1-1951.
- [14] W. R. Anderson. Heats of formation of HNO and some related species. *Combust. Flame*, vol. 117, 1999, pp. 394-403. doi: 10.1016/S0010-2180(98)00077-7.